

Cobalt Doped Orthorhombic LiMnO_2 as Cathode Materials for Lithium-Ion Batteries

Seung-Taek Myung, Shinichi Komaba*, Naoaki Kumagai, and Koutarou Kurihara

Department of Chemical Engineering, Faculty of Engineering, Iwate University, 4-3-5 Ueda, Morioka, Iwate 020-8551

(Received July 23, 2001; CL-010685)

Orthorhombic type $\text{LiCo}_x\text{Mn}_{1-x}\text{O}_2$ ($0 \leq x \leq 0.14$) oxides have been synthesized by hydrothermal treatment of $(\text{Co}_x\text{Mn}_{1-x})_3\text{O}_4$ precursors and LiOH aqueous solution at 170°C . As-synthesized powders showed well-ordered $\beta\text{-NaMnO}_2$ structures, and the products were single crystalline particle oxides from TEM observations. The particle size decreased with increasing the amount of Co substituent. Much more improved capacity upon 100 cycling was clearly seen in orthorhombic $\text{LiCo}_{0.1}\text{Mn}_{0.9}\text{O}_2$, comparing to orthorhombic LiMnO_2 .

Orthorhombic layered LiMnO_2 (space group of $Pnmm$, hereafter referred as to $o\text{-LiMnO}_2$) which has a zigzag layered $\beta\text{-NaMnO}_2$ structure is expected to work as 3 V class cathode material for Li-ion secondary battery. It was reported that electrochemical behavior of $o\text{-LiMnO}_2$ is highly dependent on its crystallite size.¹ Wet-process has advantages to synthesize homogeneous oxide powders. Low-temperature solution technique seemed to be necessary to obtain high capacity upon cycling.^{2,3}

However, it was known that powder preparation of $o\text{-LiMnO}_2$ is not so easy, that is, necessity of well controlled oxygen or reduction atmosphere.⁴ To simplify $o\text{-LiMnO}_2$ preparation, hydrothermal reaction is very attractive method to achieve relatively low temperature synthesis.⁵⁻⁷ Recently, we have successfully prepared high crystalline $o\text{-LiMnO}_2$ by hydrothermal treatment of Mn_3O_4 with LiOH aqueous solution.⁷ Other research groups tried to substitute Mn sites in $o\text{-LiMnO}_2$ by other elements such as Al^{8,9} and Cr¹⁰, and the products resulted in monoclinic LiMnO_2 structure crystallization because of unstability of other elements doped $o\text{-LiMnO}_2$ as simulated by Ceder et al.¹¹ To our knowledge, only $\leq 5\%$ of replacement of Mn site in $o\text{-LiMnO}_2$ system ($\beta\text{-NaMnO}_2$ structure) was reported.⁸⁻¹⁰ Here, we have succeeded to substitute a part of the manganese site with Co in $o\text{-LiMnO}_2$ by the hydrothermal treatment of Co doped Mn_3O_4 . This technique will be applied to various elements doping in $o\text{-LiMnO}_2$. The products were crystallized in a well-ordered $\beta\text{-NaMnO}_2$ system. We investigated powder and electrochemical properties of $o\text{-LiCo}_x\text{Mn}_{1-x}\text{O}_2$ ($0 \leq x \leq 0.14$).

$(\text{Co}_x\text{Mn}_{1-x})_3\text{O}_4$ ($0 \leq x \leq 0.5$) as hydrothermal reaction precursors were synthesized through a mild autoxidation route.^{7,12} Manganese acetate tetrahydrate ($\text{Mn}(\text{CH}_3\text{COO})_2 \cdot 4\text{H}_2\text{O}$) and cobalt acetate tetrahydrate ($\text{Co}(\text{CH}_3\text{COO})_2 \cdot 4\text{H}_2\text{O}$) were dissolved in distilled water. The prepared precursors were hydrothermally treated with 3.5 M of LiOH aqueous solution at 170°C for 4 days in teflon-sealed autoclaves. Details of powder preparation sequence are described in our previous reports.^{7,13} The XRDs were precisely taken with a step of $0.003^\circ \text{s}^{-1}$ to detect any impurity phase. To analyze chemical composition of the products, atomic absorption analyses (AAAnalyst 300, Perkin Elmer, USA) were carried out. Cathodes were prepared by blending the hydrothermally prepared oxide powders, graphite, acetylene black and PVDF (80:5:10:5) in NMP. The slurry was pasted on Ni ex-met, and dried for 1 day at

120°C , and then pressed. The dried electrodes were dried again for 4 days at 80°C in a vacuum state oven. A beaker-type cell consisted of the cathode as working electrode and lithium foil as a counter electrode was assembled in an Ar-filled glove box. The used electrolytes was 1M LiClO_4 in EC : DEC (1:1).

$(\text{Co}_x\text{Mn}_{1-x})_3\text{O}_4$ ($0 \leq x \leq 0.5$) as hydrothermal reaction precursors were formed by oxidation of $\text{Co}_x\text{Mn}_{1-x}(\text{OH})_2$ at 80°C . $(\text{Co}_x\text{Mn}_{1-x})_3\text{O}_4$ phase having a space group $I4_1/amd$ appears as the major phase with no other Mn-containing minor phase being detectable. During hydrothermal reaction of $(\text{Co}_x\text{Mn}_{1-x})_3\text{O}_4$ in LiOH aqueous solution, the precursors phases were gradually changed to $o\text{-LiMnO}_2$ phase.^{7,13} The details of the phase evolution steps are described in Reference 13. As can be seen in XRD patterns in Figure 1, all peaks can be indexed as $o\text{-LiMnO}_2$, and the $(\text{Co}_x\text{Mn}_{1-x})_3\text{O}_4$ phase ($I4_1/amd$) was not detected in the products. In case of high temperature calcination, the oxidation state of Mn would be readily more than 3, giving rise to such lithium excess or deficient phase as Li_2MnO_3 or LiMn_2O_4 .^{8,9,14} The problem was solved by employing hydrothermal treatment in this study. From AAS measurements (Table 1), it can be seen that the products have desired compositions. The calculated lattice parameters decrease gradually with increasing Co content. Hence, one can understand that solid solution in $o\text{-LiMnO}_2$ system was formed up to $x = 0.14$ in $\text{LiCo}_x\text{Mn}_{1-x}\text{O}_2$. It is likely that the substitution of the small Co^{3+} ion for the larger Jahn–Teller distorted Mn^{3+} ion in the host structure results in a contraction of the lattice.

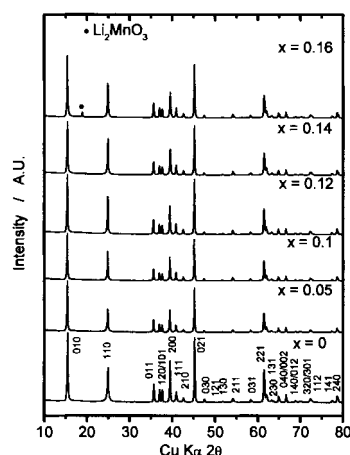


Figure 1. XRD patterns of Co doped $o\text{-LiMnO}_2$ as a function of Co doping amount, x in $\text{LiCo}_x\text{Mn}_{1-x}\text{O}_2$.

With increasing Co doping amount, simultaneously, FWHMs of the (110) peaks are getting smaller down to $x = 0.14$ in $\text{LiCo}_x\text{Mn}_{1-x}\text{O}_2$. The stronger bonding energy of Co–O in Mn–O octahedral environment of $\text{LiCo}_x\text{Mn}_{1-x}\text{O}_2$ structure is probably attributable to increase in the symmetry of the (110) plane, leading to the enhanced structural integrity. Therefore, it was thought that the sharpening of the (110) diffraction peak not only confirms the

Table 1. Variations in lattice parameters, FWHMs and their corresponding chemical compositions as a function of Co doping amount

x in $\text{LiCo}_x\text{Mn}_{1-x}\text{O}_2$	a/Å	b/Å	c/Å	Volume/Å ³	FWHM (2θ/°) ^a	Chemical composition
0	4.5795	5.7550	2.8106	74.0733	0.635	$\text{Li}_{1.03}\text{Mn}_{1.00}\text{O}_2$
0.05	4.5764	5.7541	2.8094	73.9801	0.353	$\text{Li}_{1.00}\text{Co}_{0.06}\text{Mn}_{0.94}\text{O}_2$
0.1	4.5751	5.7537	2.8093	73.9513	0.212	$\text{Li}_{1.00}\text{Co}_{0.10}\text{Mn}_{0.90}\text{O}_2$
0.12	4.5748	5.7535	2.8092	73.9413	0.176	$\text{Li}_{1.00}\text{Co}_{0.12}\text{Mn}_{0.88}\text{O}_2$
0.14	4.5743	5.7532	2.8091	73.9267	0.141	$\text{Li}_{1.00}\text{Co}_{0.14}\text{Mn}_{0.86}\text{O}_2$

^aFull width of half maximum (FWHM) of (110) Bragg peak.

presence of the substituent ion in Mn sites of *o*-LiMnO₂, but also should provide further evidence for a much ordered local coordination symmetry of the substituted structure.

In general, when more than 5% of other elements (Al, Cr) are doped in manganese site, ordered *o*-LiMnO₂ undergoes structural variation toward monoclinic faulted LiMnO₂ structure, because the monoclinically distorted LiMnO₂ is thermodynamically more stable than orthorhombic structured LiMnO₂.¹¹ In our experiment, however, a new hydrothermal condition results in a well-ordered Co doped *o*-LiMnO₂, and the solid solution limit by hydrothermal approach is $x \leq 0.14$ in *o*-LiCo_xMn_{1-x}O₂.

The charge and discharge characteristics of Li/*o*-LiMnO₂ and Li/*o*-LiCo_{0.1}Mn_{0.9}O₂ cells in the voltage range of 2.0–4.3 V_{Li/Li⁺} at a current density of 0.1 mA cm⁻² (ca. 45 mA g⁻¹) are shown in Figure 2; corresponding specific charge–discharge curves are given in Figures 2(a) and (b). The cells initially exhibit a single charging voltage plateau, and the initial charge capacity increased about 45 mA h (g-oxide)⁻¹ by Co doping. While a large capacity loss during the first discharge was seen in both samples. According to our ex situ XRD experiment, the both orthorhombic phases were electrochemically converted into a spinel like phase at the potential around 4.1 V_{Li/Li⁺}. As cycle goes by, the 4 V plateaus of the spinel like phase were developed more and more in the both

cells, resulting in increased discharge capacities (Figures 2(a) and (b)). The crystallinity of the spinel-like phase became progressively higher with further cycling confirmed by ex situ XRD, which is close to Reference 4. That means that full spinel transformation by electrochemical reaction is necessary to obtain higher capacity.

Obviously, the orthorhombic structure was much stabilized by Co substitution on Mn sites, as described in Table 1, especially on 3 V region shown in Figure 2(b). In case of Mn-site doped conventional spinel compound, cyclability at long terms was enhanced by Mn-site replacement by other elements. However, higher level doping on Mn sites resulted in decrease in obtained capacity, even though the cyclability is better than lower level one. We think that the fact is applicable to orthorhombic system, because the battery performance of $x = 0.1$ in LiCo_xMn_{1-x}O₂ is superior to $x = 0$ and $x = 0.14$. Furthermore, we believe that electric conductivity of Co doped sample is higher than undoped one. This result is very similar to those of Co or Ni doped monoclinic LiMnO₂.^{15–17} These results suggest that the Co doped *o*-LiMnO₂ having higher capacity and good cyclability upon cycling is substantially more stable to cycle than the unsubstituted material.

This study was supported by NEDO of Japan and Yazaki Memorial Foundation. S.T.M. acknowledges Yoneyama studentship.

References and Notes

- 1 L. Croguennec, P. Deniard, and R. Brec, *J. Electrochem. Soc.*, **144**, 3323 (1997).
- 2 G. Pistoia, A. Antonini, and D. Zane, *Solid State Ionics*, **78**, 115 (1995).
- 3 J. N. Reimers, E. W. Fuller, E. Rossen, and J. R. Dahn, *J. Electrochem. Soc.*, **140**, 3396 (1993).
- 4 Y.-I. Jang, B. Huang, H. Wang, D. R. Sadoway, and Y.-M. Chiang, *J. Electrochem. Soc.*, **146**, 3217 (1999).
- 5 M. Tabuchi, K. Ado, C. Masquelier, I. Matsubara, H. Sakaebe, H. Kageyama, H. Kobayashi, R. Kanno, and O. Nakamura, *Solid State Ionics*, **89**, 53 (1996).
- 6 Y. Nitta, M. Nagayama, H. Miyake, and A. Ohta, *J. Power Sources*, **81–82**, 49 (1999).
- 7 S.-T. Myung, S. Komaba, and N. Kumagai, *Chem. Lett.*, **2001**, 80.
- 8 Y.-M. Chiang, D. R. Sadoway, Y.-I. Chiang, B. Huang, and H. Wang, *Electrochem. and Solid-State Lett.*, **2**, 107 (1999).
- 9 Y.-I. Jang and Y.-M. Chiang, *Solid State Ionics*, **130**, 53 (2000).
- 10 B. Amundsen, J. Desilvestro, T. Groutso, D. Hassell, J. B. Metson, E. Regan, R. Steiner, and P. J. Pickering, *J. Electrochem. Soc.*, **147**, 4078 (2000).
- 11 G. Ceder and S. K. Mishra, *Electrochem. Solid-State Lett.*, **2**, 550 (1999).
- 12 A. R. Nichols and J. H. Walton, *J. Am. Chem. Soc.*, **64**, 1866 (1942).
- 13 N. Kumagai, S.-T. Myung, and S. Komaba, Lithium Battery Discussion Proc., Arcachon, June 2001, Oral N° 90.
- 14 S.-T. Myung, S. Komaba, and N. Kumagai, *Chem. Lett.*, **2001**, 574.
- 15 T. E. Quine, M. J. Duncan, A. R. Armstrong, A. D. Robertson, and P. G. Bruce, *J. Mater. Chem.*, **10**, 2838 (2000).
- 16 A. D. Robertson, A. R. Armstrong, A. J. Fowkes, and P. G. Bruce, *J. Mater. Chem.*, **11**, 113 (2001).
- 17 A. R. Armstrong, A. D. Robertson, R. Gitzendanner, and P. G. Bruce, *J. Solid State Chem.*, **145**, 549 (1999).

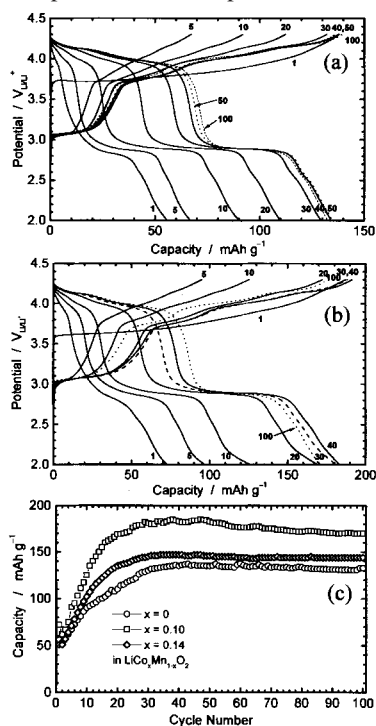


Figure 2. Charge-discharge profiles of (a) *o*-LiMnO₂, (b) *o*-LiCo_{0.1}Mn_{0.9}O₂ and (c) their cyclability at 25 °C